T.C.

ALTINBAS UNIVERSITY

Institute of Graduate Studies

Information Technologies

INTELLIGENT IDENTIFICATION SYSTEM BASED ON IRIS PATTERN RECOGNITION

Khalid Mansur ABDULAZEEZ

Master of Science

Supervisor
Asst. Prof. Dr. Sefer KURNAZ

Istanbul, 2021

INTELLIGENT IDENTIFICATION SYSTEM BASED ON IRIS PATTERN RECOGNITION

by

Khalid Mansur ABDULAZEEZ

Information Technologies

Submitted to the Institute of Graduate Studies

in partial fulfillment of the requirements for the degree of

Master of Science

ALTINBAS UNIVERSITY

2021

The thesis titled “INTELLIGENT IDENTIFICATION SYSTEM BASED ON IRIS PATTERN RECOGNITION” prepared and presented by “Khalid Mansur ABDULAZEEZ” was accepted as a Master of Science Thesis in Information Technologies.

____

Asst. Prof. Dr. Sefer KURNAZ

Supervisor

Thesis Defens Jury Members:

Asst. Prof. Dr. Sefer KURNAZ	School of Engineering and Natural Sciences, Altinbas University	________________
Prof. Dr. Osman Nuri UÇAN	School of Engineering and Natural Sciences, Altinbas University	________________
Asst. Prof. Dr. Zeynep ALTAN	Faculty of Engineering and Architecture, Beykent University	________________

I certify that this thesis satisfies all the requirements as a thesis for the degree of Master of Science.

Approval Date of Institute of Graduate Studies:

____/___/____

I hereby declare that all information in this document has been obtained and presented in accordance with academic rules and ethical conduct. I also declare that, as required by these rules and conduct, I have fully cited and referenced all material and results that are not original to this work.

Khalid Mansur ABDULAZEEZ

DEDICATION

First and foremost, I would like to thank Allah Almighty for giving me the knowledge, ability and opportunity to undertake this research study and to persevere and complete it satisfactorily. Heartfelt thanks goes to my father and my mother. Every success is a direct consequence of their influence in my life and their love. At the end I have to mention my brother and sister for their support and love.

ACKNOWLEDGEMENTS

All praises are to ALLAH Subhanahu wa Ta'aala for bestowing me with health, opportunity, patience, and knowledge to complete this research. May the peace and blessings of ALLAH Subhanahu wa Ta'aala be upon Prophet Muhammad (Sallallahu alayhi wa sallam). My profound gratitude goes to my supervisor Asst. Prof. Dr. Sefer KURNAZ, for his invaluable guidance, excellent supervision, continuous encouragement and constant support in making this research possible. His cooperation, tolerance, constructive criticism and useful suggestions have been of immense encouragement to me and enabled me to develop a deeper understanding of this research. I also thank Dr. Alaa Hamid Mohammed I sincerely thank him for the time spent in proofreading and correcting my mistakes. Finally, I extend my gratitude to all those who were directly or indirectly involved by either encouraging, praying and offering constructive advice in this thesis.

Thank you.

ABSTRACT

INTELLIGENT IDENTIFICATION SYSTEM BASED ON IRIS PATTERN RECOGNITION

ABDULAZEEZ, Khalid Mansur

M. Sc., Information Technologies, Altinbas University

Supervisor: Asst. Prof. Dr. Sefer KURNAZ

Date: 05/2021

Pages: 49

The identification process is one of the important processes to achieve safety, which is used daily in many areas such as the attendance system, various Internet or social sites, personal accounts inside banks and other important areas. In this article, the model is a genuine model mode as a marker of the character of the individual suggested on the SIFT technique. To tackle identity theft, poor picture quality, noise and volatility of the ambient world, we have defined the iris patterns and features for each person. The Hamming distance algorithm was used on a dataset of 50 individuals to figure out how close new entrants to the dataset ought to be to a current person's entry. 98% of the value, the bogus assent rate, and the refusal pace of 0.15% and 0.25%, separately, yielded the aftereffects of the application strategy.

KEYWORDS: Iris Identification System, Computer vision, Pattern Recognition, SIFT, Multi-model Bio Centric System.

TABLE OF CONTENTS

Pages

LIST OF TABLES

Pages

LIST OF FIGURES

Pages

LIST OF ABBREVIATIONS

CDR:	Cup-to-Disc Ratio
DR:	Diabetic Retinopathy
DRIVE:	Digital Retinal Images for Vessel Extraction
MESSIDOR	Methods to Evaluate Segmentation and Indexing
OD:	Optic Disc
STARE:	Structured Analysis of the Retina

1. INTRODUCTION

1.1 OVERVIEW

Now, security plays an essential role in any company to avoid bad practices such as information theft, replacement of real data, unauthorized entry of a restricted area, etc. To defeat such types of misconduct, they resort to strict security measures using authentication and delegation. There are many kinds of authentication technologies, classified into three principal sections:

- Something you remember (e.g. a password)
- Something you own (like an ATM card)
- Something that you are (known as biometrics)

Human physiological or behavioral features can be used to verify the biometrics. There are many circumstances to consider when determining the right biometrics for an application like Global. That means that every user can add their parties to the system. The uniqueness, which indicates that this trait is there to differentiate between people, means that this function does not change over time. Scalability implies an accessible collection and measurement of this trait.

The data must be such that the processing and removal of relevant function sets and the consequent achievement are possible. Means accuracy, speed, technological durability, and acceptance; That is, how individuals accept this technology (they are ready to capture and evaluate their biometrics), bypassing; It refers to the ease with which any imaginary (artificial) property can be negated.

Biometric methods have been used in forensic abilities. Nowadays, it is used for civil applications, e.g., B. control of physical access to installations, control of logical access to programs, and voters' monitoring during elections.

Iris identification is a biometric authentication system that works profiling procedures on images of the eye's iris to identify a person. The iris symbol has been issued in commercial iris identification operations for various security applications. Over 50 million people have registered with the Iris Code.

The iris recognition system, due to its stability, uniqueness and non-invasive properties, is the most reliable system in high security environments compared to other biometric technologies such as (palm veins, fingerprint, signature, handprint, iris, etc.). The iris symbol is a group of bits. Both indicate whether a tape-traced fabric filter applied to a specific point in the iris image gave a non-negative or negative result.

The iris features, unlike facial and fingerprint features, are derived from dispersed features that range from individual to person. Individual irises and identical twins can be entirely different in their shapes, yet on the opposite side of the body, you can see the same human.

Another characteristic that cannot be faked is its responsiveness. The modern cameras for capturing the iris are less invasive than previous iris scanners. Iris recognition is a powerful and safe system. Iris has unique personalities with little variation over the course of her life.

Iris contains different unique patterns that remain fixed throughout a person's life. The iris pattern can be extracted from the eye photo template. This biometric template includes illustrative information on individual irises for matching with other models. Image processing techniques are used to change the characteristics of the iris into a unique code that is recorded in the database for comparison with other templates. Iris functions are managed and stored using iris images as follows: [8]:

1. Take the photo: Take a picture of the iris with reasonable accuracy and eminence.
2. Separation: The procedure of mining the iris from an image of the eye.
3. Normalization: The characteristic of extraction and coding.
4. Save the mined symbols in the DB and associate them with the iris images.

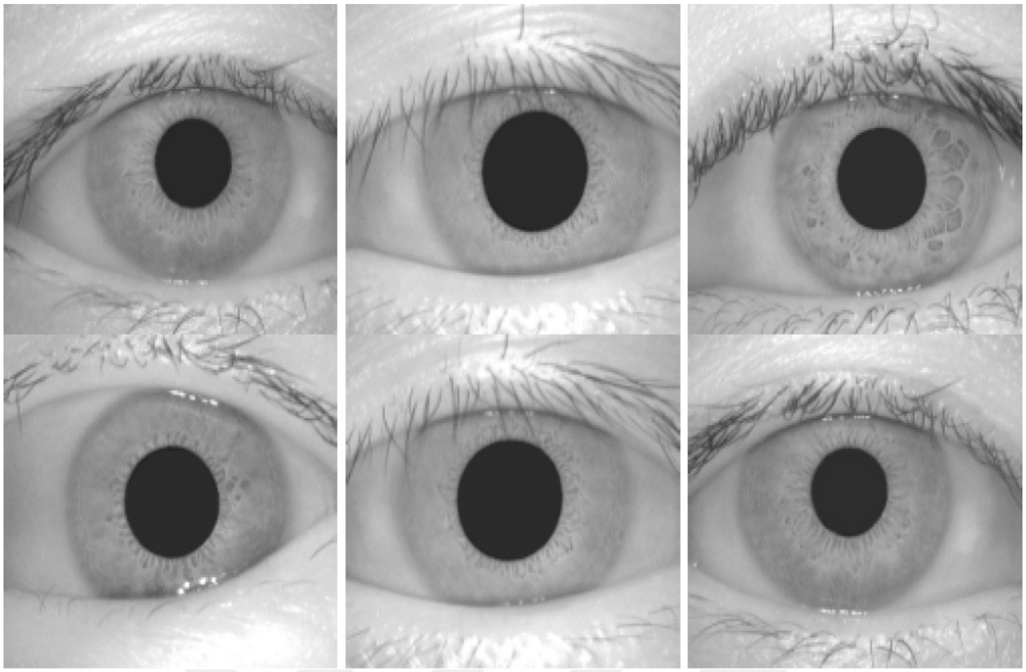

Figure 1.1: Iris Samples

The iris identification system is used to avoid illegitimate access and to identify users who are using the facility. During installation, users straightened their irises through the system. For each recorded iris image, a different iris symbol is generated and stored in the system. As soon as the user has registered the iris in the system, it will be recognized. Iris recognition offers precise uniqueness verification without the use of PINs, cards or passwords. The registration procedure takes less than 3 minutes and the verification procedure takes about 2 seconds.

Biometrics identification systems depend on individual physical characteristics. The registration and recognition procedures are the core operations of the structures above. The four sub-processes of admission or registration are as follows. This example is likewise like the finger or iris. The definition segment is the second sub-segment, including displaying test quality and commotion handling issues.

The third step-deduction is the extraction and determination of genuine human models utilizing deduction and flagging calculations like Scale Invariant Feature Transform (SIFT), Power Surveillance Machine (SURF). If this stage is complete, features that have been chosen will be placed in the database as seen in fig 1. Furthermore, the detection process, which involves sub-processes such as sampling and matching samples, may be interpreted as an iterative process. Like the sample registration method seen in Figure 1.2: this operation includes holding and matching the sample instead of logging it.

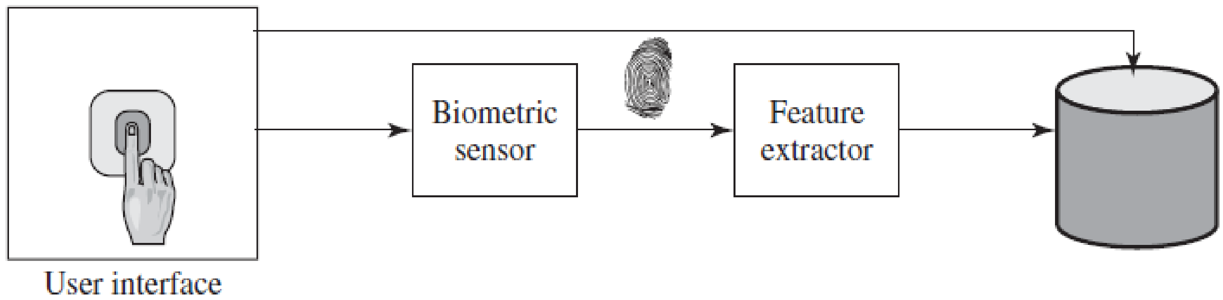

Figure 1.2: Enrollment Operation for single biometric system

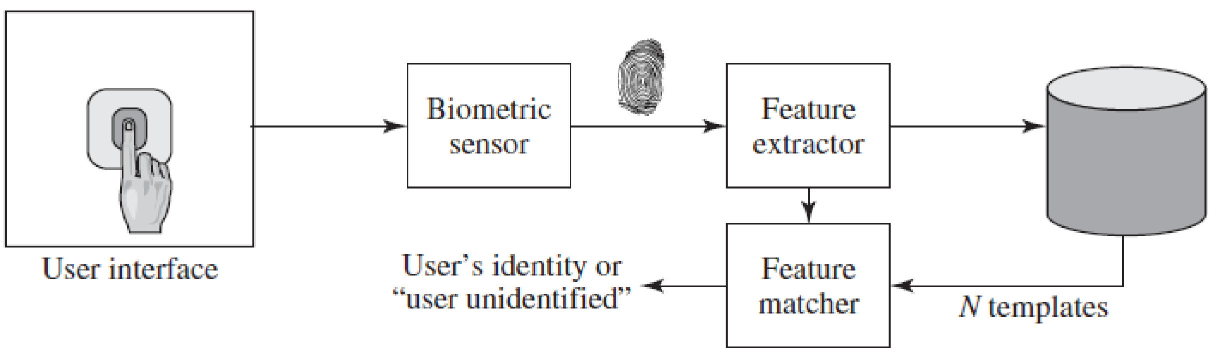

Figure 1.3: Identification Operation for single biometric system

1.2 PROBLEM DEFINITION (OR MOTIVATION)

Presently there are new strategies for human science and science that cannot be hoodwinked, taken or failed to remember. There are a wide range of ways and methods to separate between various individuals like language, iris, eye detail, DNA, fingerprints, finger muscles, and other comparative attributes of every individual. Biometrics systems were used in forensic science previously, but now their applications have expanded to include many different civil fields. In this type of measurements, there are also many challenges such as noise in the surrounding environment during enrolling sample, or poor quality of the sample or image [1].

1.3 THESIS OBJECTIVES

This essay groups the submissions into four major sections which can be outlined as follows:

- The intelligent single-modal iris identifying device in different conditions is proposed and evaluated.
- Efficient pre- and segmentation methods are employed to resolve the noise and weak photos.
- Intelligent and quick extraction and selection of features (SIFT) algorithms are used to choose different features between samples.
- In the final step, the hammer distance is used as the algorithm for models that fit the SVM to approve or deny the consumer in the recognition process.

1.4 THESIS SCOPE

The suggested system is biometric system using iris patterns. There are three related stages in the proposed method. The first step is the iris registration phase, which involves three phases such as pre-processing, removing functionality and the data base storage template. The second step is defining, checking and mixing. The purpose of the suggested model is to improve the precision of a single biometric device by another model. The third last stage is the score-level fusion process.

1.5 DOCUMENT STRUCTURE

This work consists of six parts. These parts are prepared to imitate the technical steps towards our main goal. A brief explanation of the content of each part can be found in the following:

- In the first chapter, the thesis goals, the motivation behind the thesis, the approach used in the thesis, the thesis contribution, the scope of work, and the thesis planning are presented.
- Part II gives the reader an overview of the literature review.
- Part III provides an analysis of the system and user requirements.
- Part V introduces system design and UML diagrams.
- Part IV introduces the system implementation and screenshots of system icons and system results.

Finally, the conclusions and future work are presented in Chapter 6.

2. LITERATURE REVIEW

2.1 INTRODUCTION

The basic biological characteristic features of any individual are saved in a template in any biological scheme, particularly biometrics, and then compared to the template before it is presented in the identification method.

Therefore, not all biological measurements are biometric whether they include such essential characteristics like universality (UV), distinctive characteristics, permanence (PM) and weakness. This biometrics form can be generalized to all users with the Universality factor (UV). Unique factor (UQ) implies that for these biometric measurements every two individual cannot and does not have equivalent patterns.

Permanence Factor (PM) ensures that trends or biometrics of this sort cannot alter with time. Exhibits of biological measurements are hair color or body weight, but alter with time, and we cannot deem them accepted biometric measures.

The compression by some important features across various types of biometrics is performed in Table 1. Table 1 shows we had very trained features of Iris and Finger vein which were to be incorporated into a multimodal framework.

Table 1.1: Compression by usability factors between various forms of biometrics

Factors	Fingerprint	Face	Iris	Finger Vein	Voice
Universality	2	2	2	1	2
Distinctiveness	2	2	2	2	1
Permanence	2	0	2	2	0
Performance or Accuracy	0	1	2	1	0
Vulnerability (Spoofing)	2	1	0	0	2
Security	0	1	2	2	0

2 – high

1 – Medium

0 – Low

After biometric methods, implications, and relevance to security, many researchers make it challenging to develop a robust, secure, and compliant method in an environment of limited discoveries.

2.2 BACKGROUND

You should provide a brief section giving background information on the materials needed to follow your project because the information and experience of the readers with the subject and materials involved may vary.

2.2.1 Color Histogram as (feature-based algorithm)

They share a pixel value-based signature for each picture which set the foundation for comparison. However, only the color signature for photo recuperation is included. General image color recovery systems, as used in the extraction process, can be categorized into three categories: histogram, color mapping and area-based scan. Two color spaces analyze graph-based analysis methods.

A color space is described in the form of intensity values as a model to show a color. A color space usually describes a spectrum between one and four measurements. Just two 3D color spaces, rot, green and blue, and HSV, are screened (hue, saturation and value).

The histogram scan differentiates a picture by its color or histogram distribution. The similarity of the color graph representations was calculated by varying histogram spacing. The most widely employed is the Euclidean interval and its variants. A strong connection with the semantics of the picture occurs in the process for indexing color cards. However, restored photos might not be semantic with the same color distribution, but with a common color scheme.

To use a good color space for a specific application, a color shift between color spaces is appropriate. Because of its strength and the separate color detail, HSV is sufficient color space than RGB. The perceived color shifts should be retained in decent color space for the photo recovery method. In other terms, the variations in figures must be around the disparity that an individual perceives. Then it is more difficult to change from the HSV region to the RGB than the equations (1), (2), (3). We have a separate equation for and sector of the color triangle owing to the color knowledge existence.

Red-Green sector

$for\ 0^{\circ} < H \leq 120^{\circ}$

$$B = \frac{1}{3}(1 - S), R = \frac{1}{3}\left[1 + \frac{S \cos H}{\cos(60^{\circ} - H)}\right], G = 1 - (r + b) \qquad (1)$$

Green-Blue sector

$for\ 120^{\circ} < H \leq 240^{\circ}$

$$r = \frac{1}{3}(1 - S), g = \frac{1}{3}\left[1 + \frac{S \cos H}{\cos(60^{\circ} - H)}\right], b = 1 - (r + b) \qquad (2)$$

Blue-Red sector

$for\ 240^{\circ} < H \leq 360^{\circ}$

$$g = \frac{1}{3}(1 - S), b = \frac{1}{3}\left[1 + \frac{S \cos H}{\cos(60^{\circ} - H)}\right], r = 1 - (r + b) \qquad (3)$$

Where H is hue, S is saturation, B is blue, R is red and G is green.

The disadvantage of displaying a general histogram is that it ignores information about its position, shape, and texture. The color diagram is irregularities with rotation, scaling, lighting differences, and image noise without any sense of human perception. Therefore, new algorithms are introduced to overcome this limitation.

2.2.2 Corner and Edge Detectors

The corner angle indicator must match the following criteria:

- Consistency: The identified positions must be insensitive to noise diversity and, above all, must not move when several images are taken from the same scene.
- Accuracy, angles should be detected as close as possible to the correct positions.
- Speed - Even the best angle detector is useless if it's not fast enough.

The Harris corner detector is a popular point-of-interest detector due to its strong stability towards rotation, scaling, and image noise are all determined by the autocorrelation function in eq (4).

Harris managed to discover the powerful features in a given image that meet the requirements that meet the first two criteria above.

$$C(x, y) = \sum_{w} [I(x_i, y_i) - I(x_i + \Delta x, y_i + \Delta y)]^2 \quad (4)$$

Where I denote the image function and (xi, yi) are the points in the window W (Gaussian1) centered on (x, y) and matrix C (x, y) captures the intensity structure of the local neighborhood.

2.2.3 SIFT

SIFT (Fixed Scale Feature Transformation) was first proposed by Lowe to perform better object recognition performance. Due to its benefits in terms of stability in terms of size, rotation, and affine transformation, SIFT is rapidly being used in many application areas, individually in biometrics. The main criterion for SIFT is to find sharp points in the scale space, filter them to get stable points, and then extract local features of the images around these fixed points so that local descriptors for matching are generated from these local features.

SIFT is divided into four principal forms: a) detection of the measurement room, b) location of the main point, c) routing assignment, and d) primary point descriptor. In the first stage, a Gaussian difference function (DOG) was used to identify potential interest points consistent in both measurement and orientation. DOG was used instead of Gauss to improve the calculation speed.

Main point localization step, points with low contrast are ignored, and the edge response is canceled. A Hessian matrix was used to calculate major bends and reduce key points whose ratio between major curves is greater than the ratio. The trend graph was formed from gradient directions of sampling points within an area around the main point to have a guiding task. According to experiments, the best results were obtained using four × four sets of graphs with eight direction fields. The SIFT descriptor used is therefore 4 x 4 x 8 = 128 dimensions.

2.3 REVIEW OF RELATED WORK

2.3.1 Single-Modal Fingerprint Identification System

Hoyle et al. [9] The proposed methods use patterns based on triple details in a hierarchical order, using not only detailed conditions but also applying mountain data to keep up the association between certain data.

[10] Kumar et al. He communicated an insubordinate demeanor towards oppressing the individuals who utilize outside advanced pictures. This paper incorporated the shortfall of a picture of the photo. To limit size contrasts, pivot, and acknowledgment of associated pictures, fingers are changed. The consequences of the test brought about 1.39% blunder.

2.3.2 Face Recognition Single Modal Solutions

There are numerous wide outcomes for top caliber from face acknowledgment model. [11] Jimenez et al. Advanced function architecture suggested for delivery of face contouring artificial prejudice. The mixture of self-configured vectors and location factors dependent on thin layer distortion is achieved with.

A groundbreaking provocation for face recognition in 2017 was launched by Apple [12]. The face recognition technology utilizes deep learning to boost identity precision continuously. The IPhone X brand has utilized this methodology and its clients think it is intense.

2.3.3 Iris Recognition Devices Single Modal

A combined framework dependent on spontaneous projecting and sporadic definitions was proposed by Pillay et al. [13]. His approach will cope with simple distortions to produce an impression of an iris. This method will result in over 96 percent production. This paper does not demonstrate machine output.

[14] Thafalingen et al. It dealt with conditions, such as image quality and iris scale, which are critical in operation. They offered unlimited registration framework requirements in smart devices. They got numerous proposals for construction. The high performance of two of these prototypes was over 97 percent. They also deliver moderate ease of use and protection.

Regas et al. [15] used an eye movement identification tool to resolve the danger presented by a falsification iris as a separation between an artificial iris and the real iris. The test findings, focused on a data collection of 200 participants, revealed that the device was able to obtain a normal ranking from 96.5% with FAR 3.4% and FRR 3.5%.

[16] Bodied et al. a method focused on the variability of the pupil size to restrict the internal feature of the iris. The pupil size changes with the strength of the light, so the vitality of the iris can be calculated on the basis of its variety. The samples were taken of 380 photos of 64 individuals in experimental experiments. The iris position efficacy of the eye samples was 98.48 per cent.

2.3.4 Modal single finger recognition system

K.R Park et al. [17] It was presented as a way of recognizing three-dimensional finger muscles with a different dimension to previous exercises. First, the localized knowledge was collected without separation of the finger muscles based on the localized double model (LBP). Finger muscles were removed on the second method of feeding. The third component is the SVM system that connects the LBP accounting values.

N. Miura et al. [18] He presented a strong procedure for eliminating the muscles of the finger. A human examination strategy that centers around the unique finger impression markers executed. Some of the time the white infrared example humiliates the abundance bone of the fingers, tissue, and muscles.

Jadhav et al. [19] It has been shown that biodegradable unique finger impression is more effective with lower creation cost, more productive than other organic structures. A best in class handling framework was utilized, which incorporated a Multi-Purpose Modeling Tool (FPGA) to work with tile models. The test outcomes were acquired by 96% and 4% FRR.

2.4 SUMMARY

Table 1.2: Comparison Overview of various forms of biometric systems by different functionality [5].

Ref.	System Type - Applied Biometric	Accuracy (S)			Usability (S)				Support Security (S)
		FAR score	FRR score	FER score	UV score	UQ score	PM score	EE score	
[9]	Single modal - Finger print	1	1	1	2	2	1	2	0
[10]	Single modal - Finger knuckle	3	3	3	2	3	3	3	0
[11]	Single modal - Face	1	1	1	3	1	1	3	1
[12]	Single modal - Face	2	2	2	3	1	1	3	3
[13]	Single modal - Iris	3	3	3	2	3	3	1	2
[14]	Single modal - Iris	3	3	3	2	3	3	1	2
[15]	Single modal - Iris	2	2	2	2	3	3	1	2
[16]	Single modal - Iris	3	3	3	2	3	3	1	2
[17]	Single modal - Finger Vein	2	2	2	2	3	3	3	3
[18]	Single modal - Finger Vein	3	1	2	3	2	2	2	2
[19]	Single modal - Finger Vein	3	2	2	2	3	3	3	3

3. METHODOLOGY

3.1 ANALYSIS OF EXISTING SYSTEMS

Iris CASIA-V1 to approximate the performance, data sets are used. The set of data comprises fifty individuals and five samples are taken in two sessions by each participant. For each module, we use four samples and a reference sample. Both samples are held in 320*280 JPG format.

3.2 REQUIREMENTS OF THE PROPOSED SYSTEM

3.2.1 Functional Requirements

- Supported Web Servers:
    - Apache server
- Processing Program:
    - MATLAB
- PHP Compatibility:
    - PHP
- Storage:
    - SQL 4.1.20 or newer

3.2.2 Non-Functional Requirements

- System Component: Back-end Server is based on a combination of system architecture and performance. We use MVC (Model, View and Controller) design pattern.
- Storage space (Database) is based on the number and capacity of the hard drives or databases built into the system. It is used to store user information such as location, personal information and product information.
- Web Service is an important part of the system design. We need API to connect to MATLAB to segment iris image and extract iris features.

3.3 PROPOSED SYSTEM ARCHITECTURE

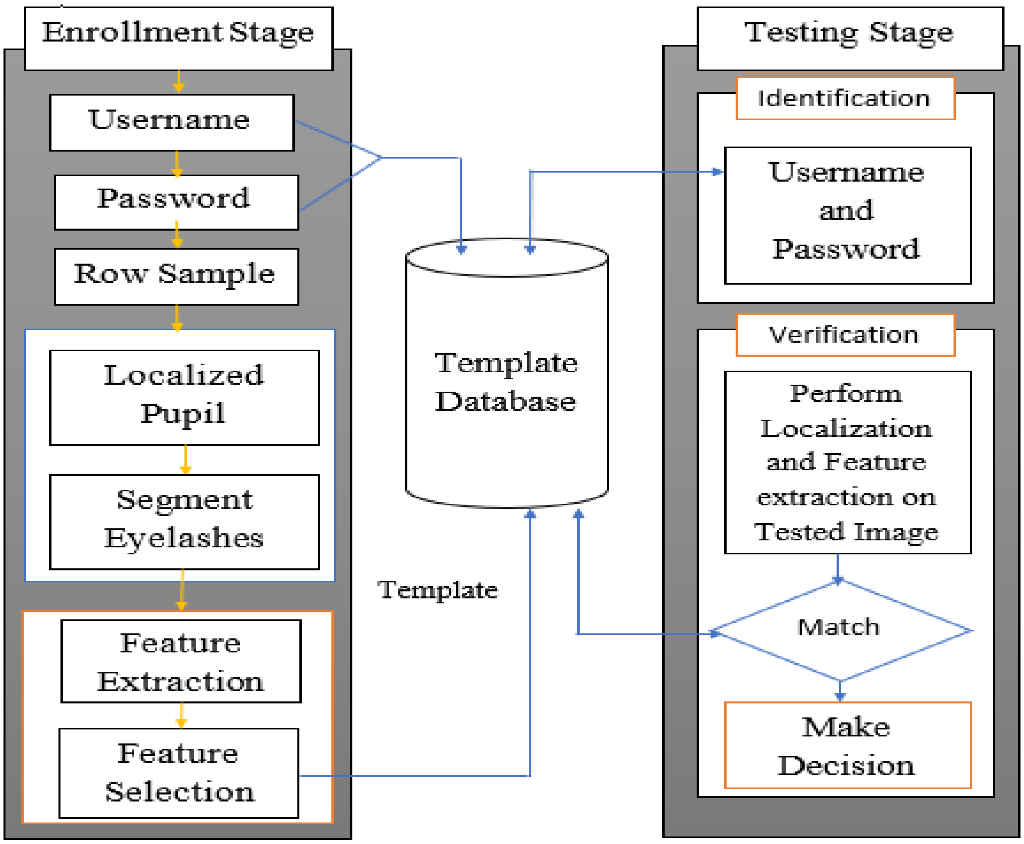

Figure 3.1: System Diagram

3.4 DEVELOPMENT METHODOLOGY

Either UML or DFD is recommended for this purpose. If you use the DFD, then use the corresponding diagrams (instead of use case and sequence diagram).

3.4.1 Use Case Diagrams

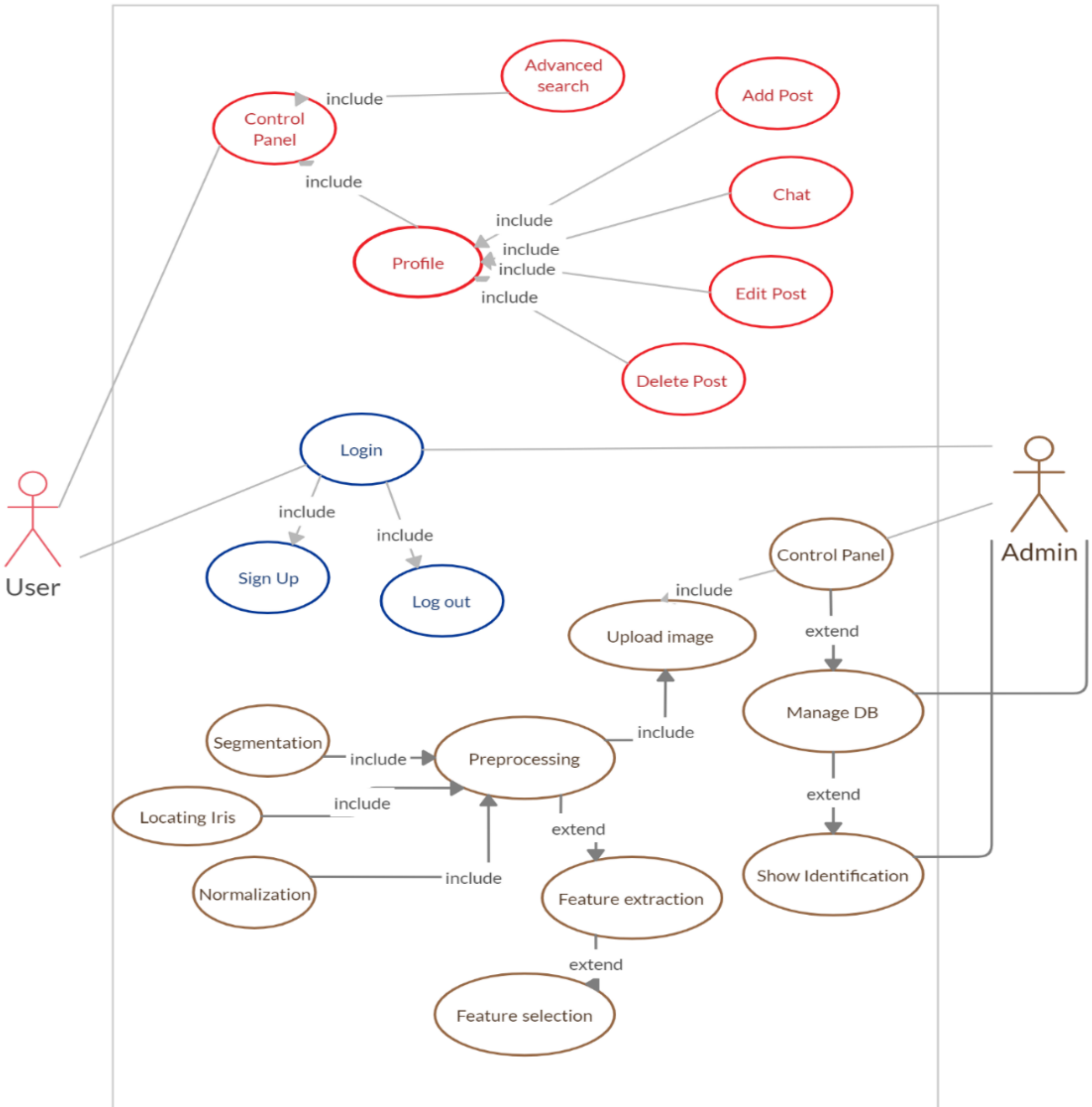

Figure 3.2: System Use case

3.4.2 Sequence Diagram

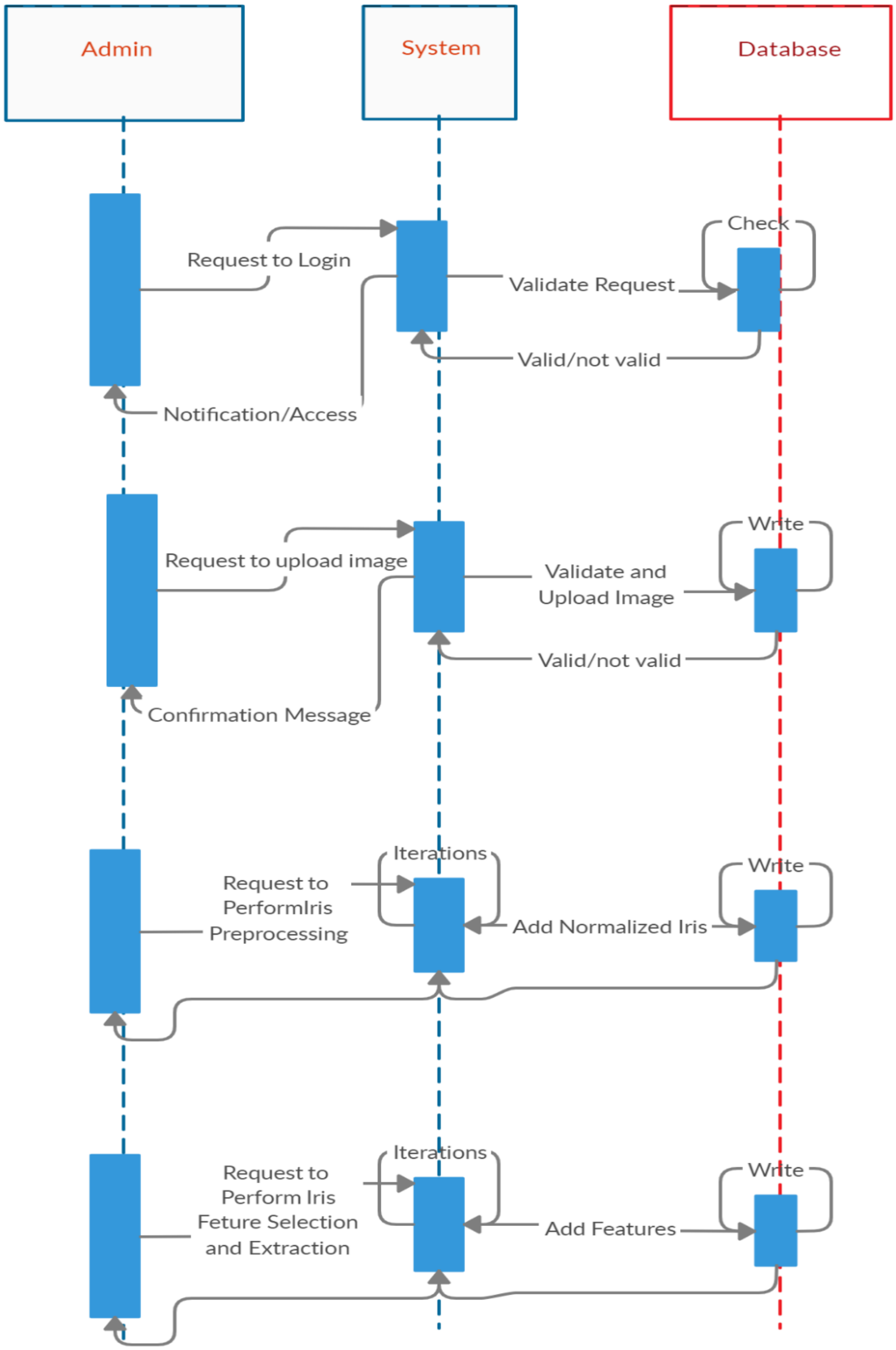

Figure 3.3: Sequence Chart

3.4.3 Activity Diagram

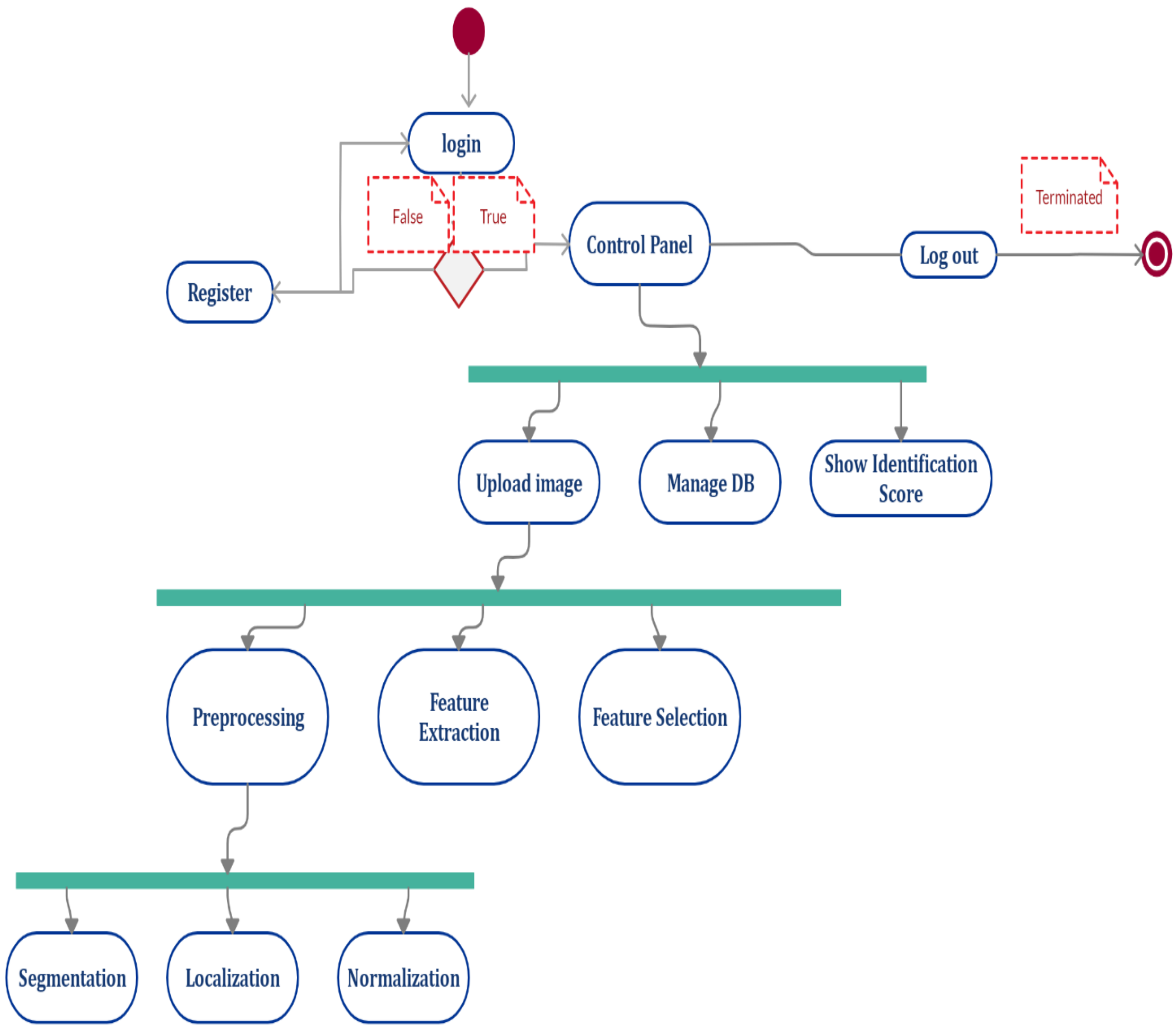

Figure 3.4: Admin Activity Chart

4. SIMULATIONS RESULTS

4.1 OVERVIEW

A single bio-model with an iris is the suggested framework as seen in Fig 3.1. There are two distinct steps in the current method. The first step is to define the iris (record) stage that consists of three steps, such as B. Pretreatment, practical method extraction and database prototype storage. The second stage is the level of contrast, which is based on the score level.

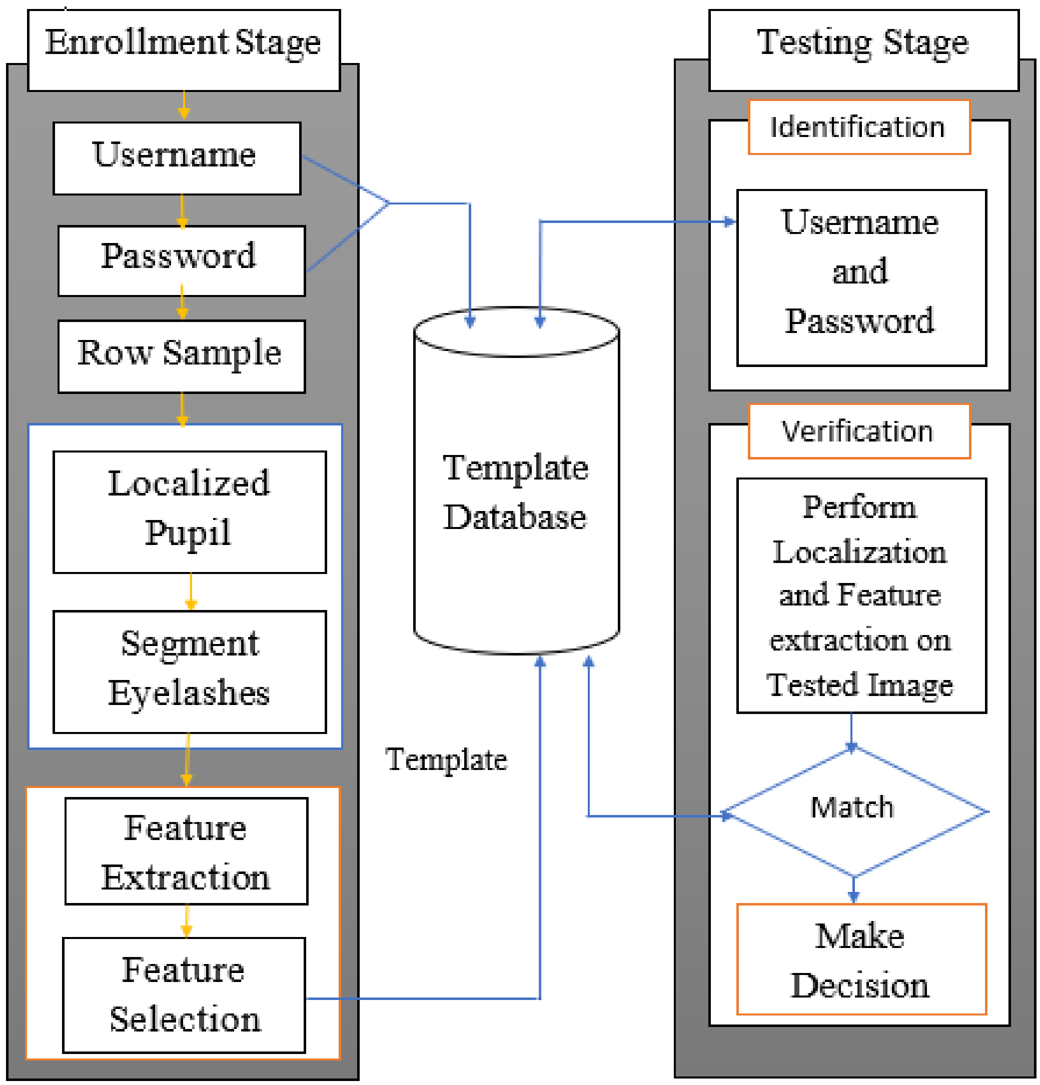

Figure 4.1: System Phases

4.1.1 Step of preprocessing

The iris recognition model at this level has two major methods, for example position and segmentation. The effects of each method are seen in fig.4.2 in the iris recognition system.

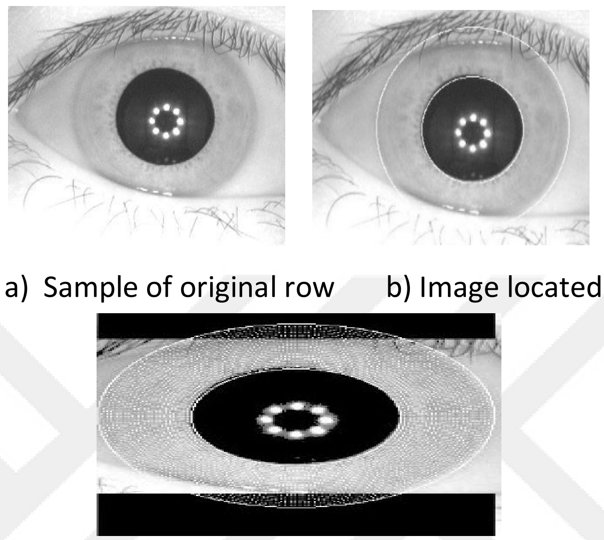

a) Sample of original row b) Image located

c) Image segmented

Figure 4.2: The results of Iris preprocessing

4.1.2 Processing of Features

Now, there are two primary territories, for example, recruiting and determination alternatives that are additionally accessible. Figure 3.3 shows the arrangement of extraction and choice of normal irises. The outcome is appeared in Figure.3.3 from each progression. We utilize distinctive extraction calculations, like SIFT, SURF, PCA, sharp point, and fast SIFT calculation.

This algorithm addresses the following noise problems in the sampling image, for example:

a) Size Challenge: Photographed or saw for size.
b) Challenge of orientation: the picture reported or checked is rotated towards each other.

c) Challenge for occlusion: incomplete coverage or interferences with another item in the recorded or checked picture.
d) Translation challenge: In a new space, like a huge or dim light volume, the speculate picture is caught or shown.

The Gaussian scale space $L(x, y, \sigma)$ of an image is represented as the convolution method $G(x, y, \sigma)$ of varying widths ¾ with the input image $I(x, y)$:

$$L(x, y, \sigma) = G(x, y, \sigma) * I(x, y) \qquad (1)$$

$$D(x, y, \sigma) = L(x, y, k\sigma) - L(x, y, \sigma) \qquad (2)$$

where k is a fixed multiplicative parameter in range space. The DoG are utilized for various purposes. Initially, it is an effective function that requires minimum calculation power to measure: The smoothed images $L(x, y, \sigma)$ require to be calculated for scale space pattern description and therefore, D can be calculated by simple subtraction. Every image sample within a 16x16 window around each key point, the gradient magnitude, m, and its orientation, θ, are computed using pixel differences:

$$\theta(x, y) = \arctan \frac{L(x,y+1) - L(x,y-1)}{L(x+1,y) - L(x-1,y)} \qquad (3)$$

Figure 4.3: Effects of iris normalization function

4.1.3 Step of matching

200 iris samples were selected from 50 individuals during the matching process; each participant has four photos during the training phase. Fifty iris samples were used by 50 individuals during the research stage. These models are gotten from the CASIA-v1 arrangement. Hamming, cosine and Euclidean are the detoxification strategies that are utilized when they are utilized. Allot the littlest space of a similar rating class on the off chance that it is underneath the limit prerequisite. Something else, there is an imprint in the diverse rating class on the off chance that it is over the base. The techniques utilized for distance are:

a) Method Euclidean Equation

$$d(x,y) = \sqrt{\sum_{i=1}^{n}(x_i - y_i)^2} \qquad (4)$$

b) Equation of Cosine Distance

$$d(x,y) = 1 - \frac{\sum_{i=1}^{n}(x*y)}{\sqrt{\sum_{i=1}^{n} x^2 * \sum_{i=1}^{n} y^2}} \qquad (5)$$

c) Equation of Hamming Distance

$$d(x,y) = \sum_{i=1}^{n} \delta(x_i, y_i) \qquad (6)$$

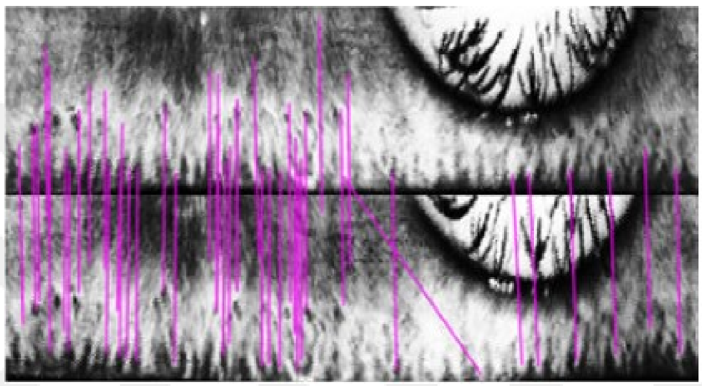

Figure 4.4: Iris matching process example Iris

4.2 INTERFACE DESIGN

4.2.1 Admin Pages

4.2.1.1 Enrolment Pages

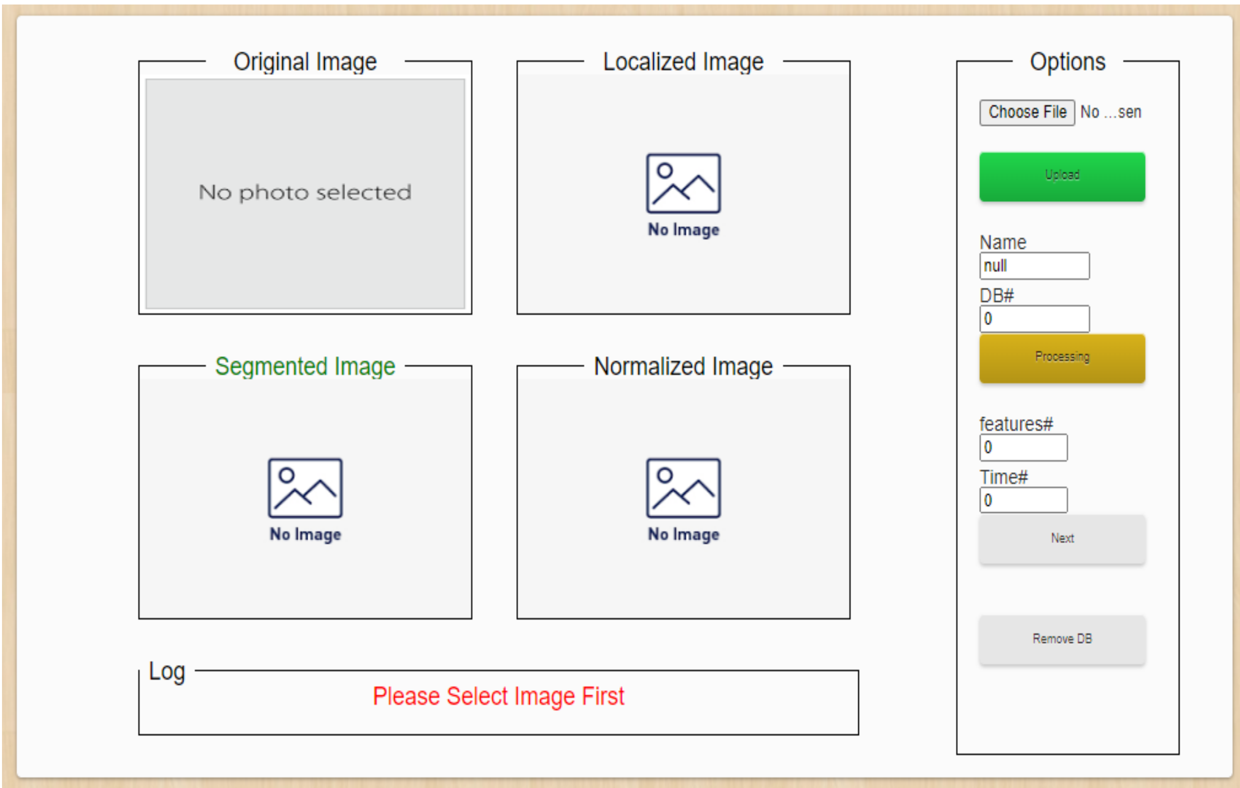

Figure 4.5: (a) Enrollment System

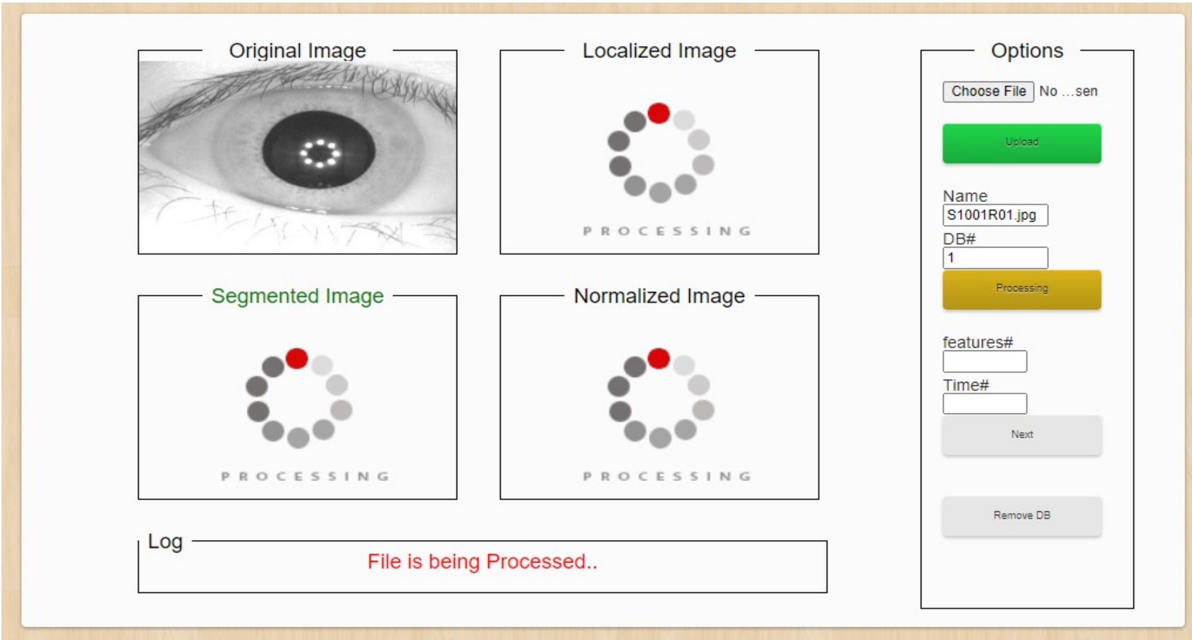

Figure 4.5: (b)Enrollment System

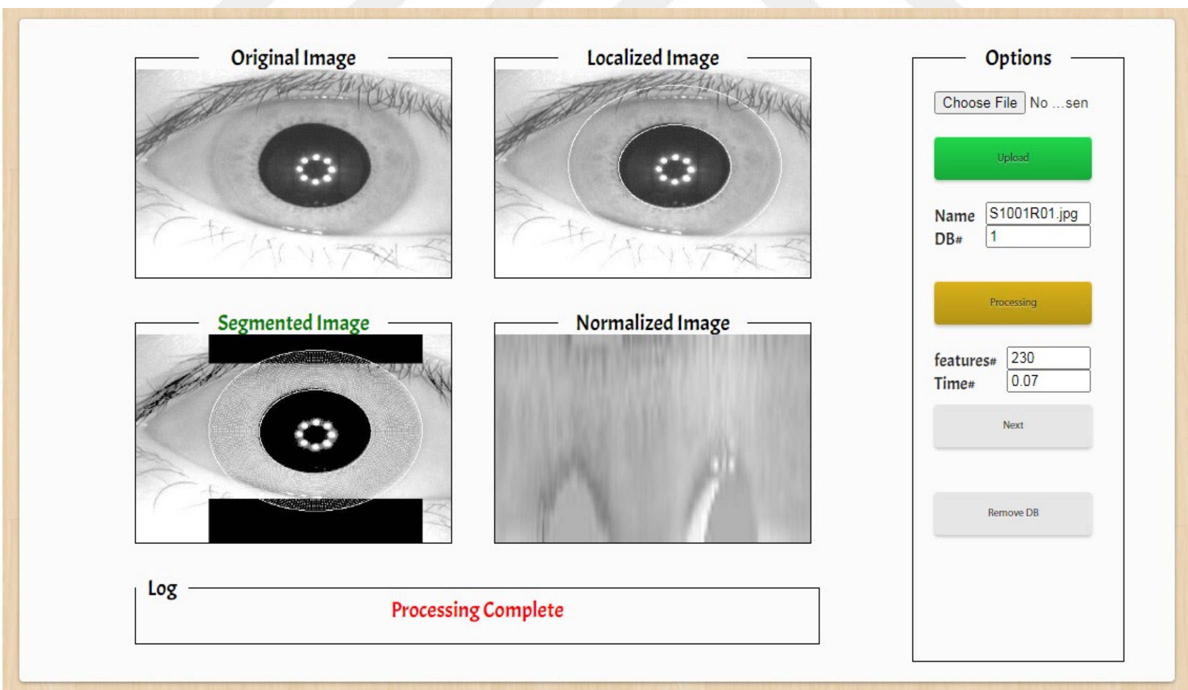

Figure 4.5: (c)Enrollment System

4.2.1.2 Testing Pages

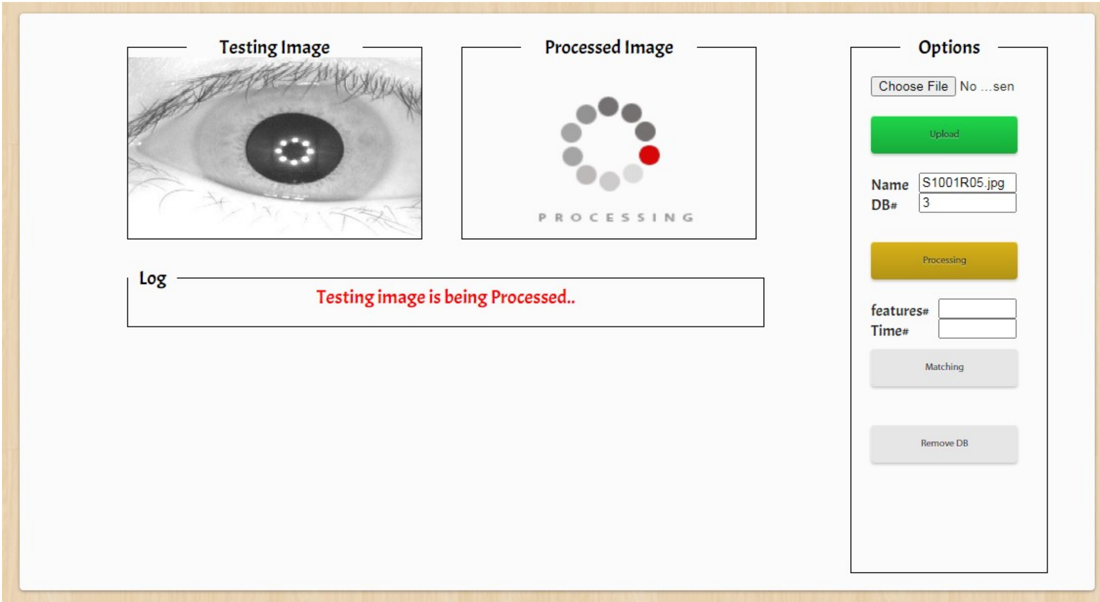

Figure 4.6: (a)Testing System

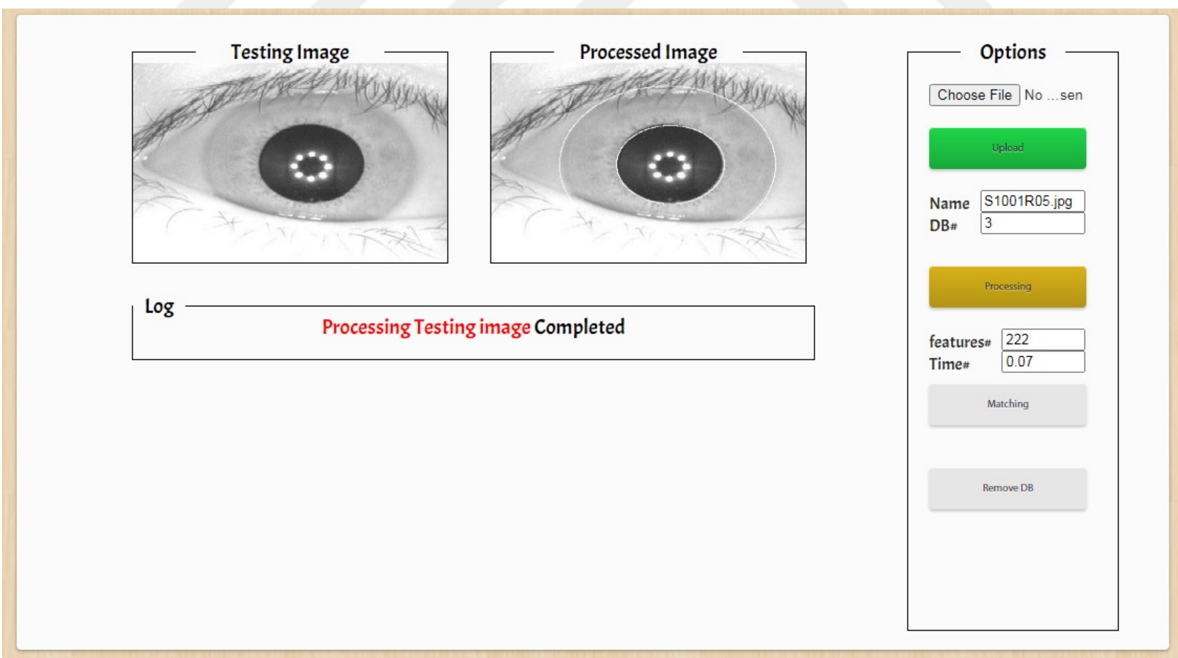

Figure 4.6: (b)Testing System

4.2.1.3 Matching Pages

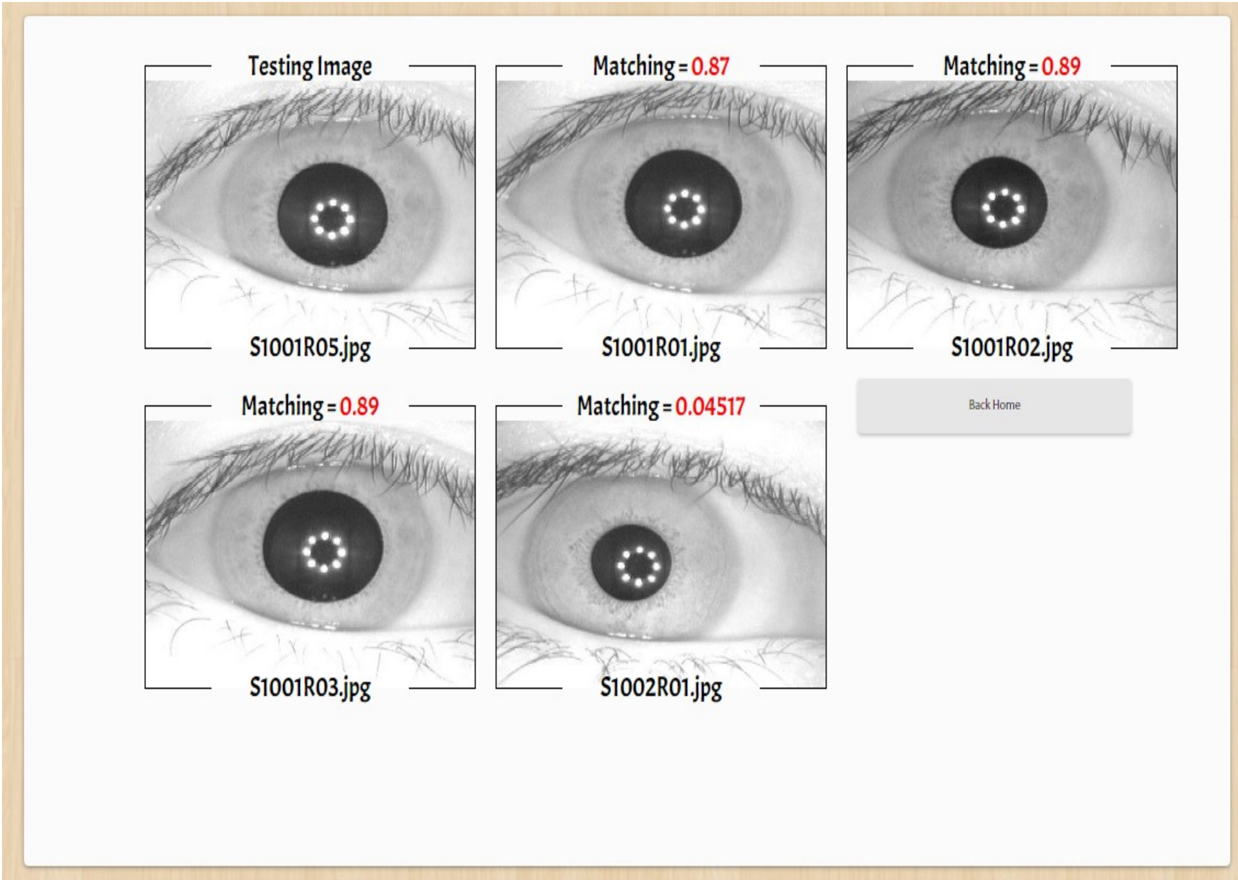

Figure 4.7: Matching System

4.2.2 User Pages

4.2.2.1 Registeration

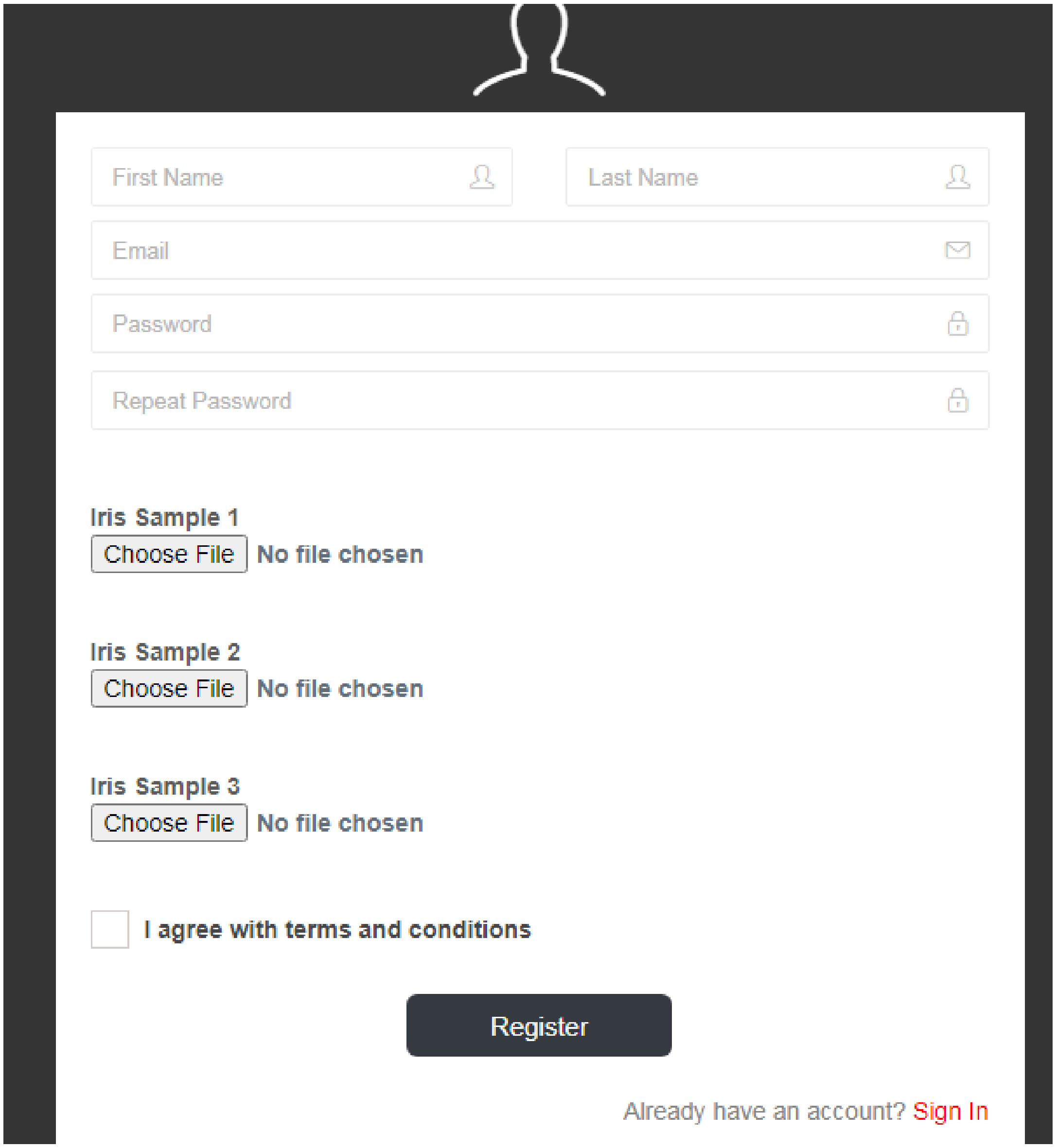

Figure 4.8: User registration System

4.2.2.2 Login

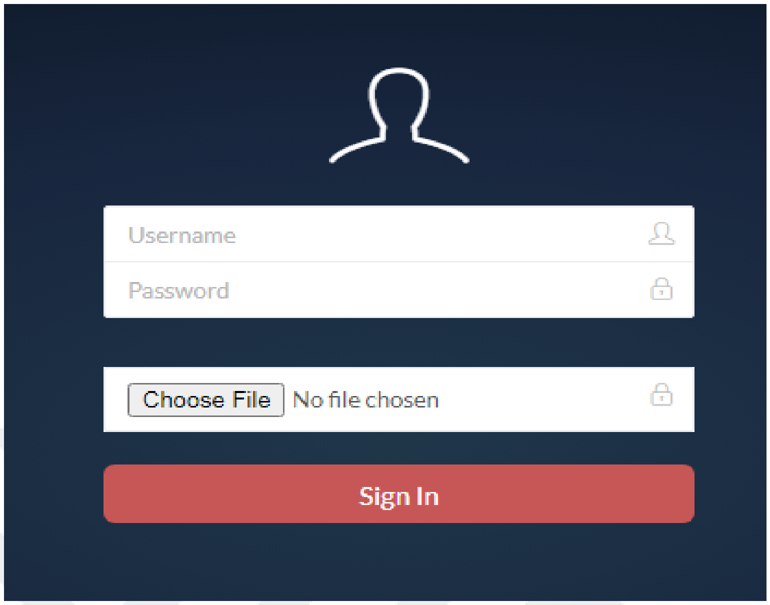

Figure 4.9: User login System

4.2.2.3 Profile Page

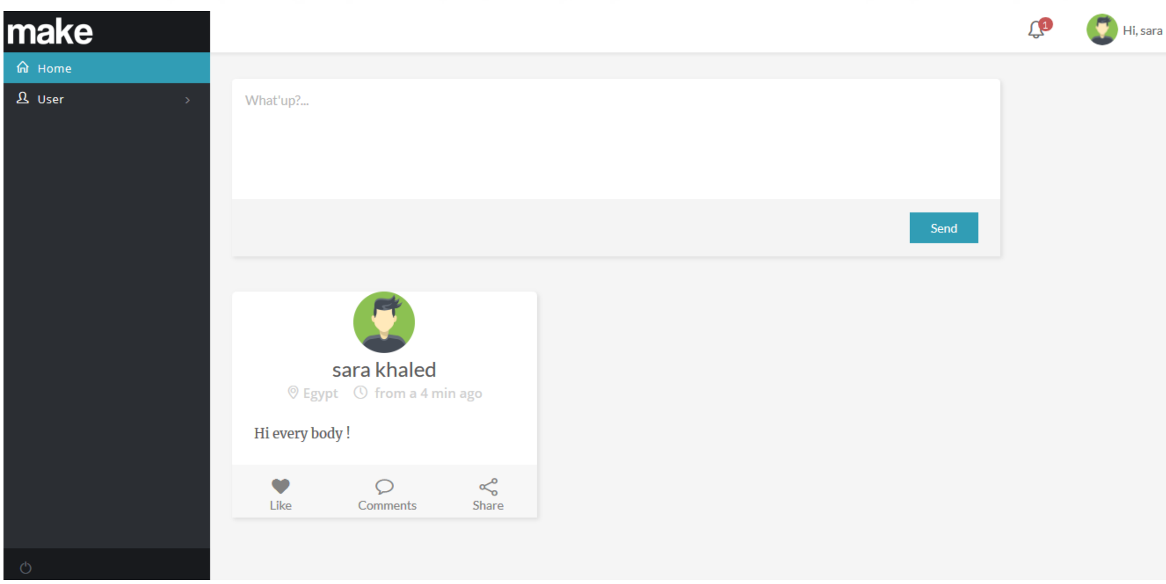

Figure 4.10: User profile System

5. SYSTEM IMPLEMENTATION

5.1 INTRODUCTION

Tests will be run on Windows 10, i7 processors, and 8GB of RAM to guarantee ideal execution and execution. To perform the tests, we use MATLAB and Apache servers. For proficient machines, MATLAB is an elite language. MATLAB is utilized to discover, benchmark, and separate Iris capacities and label them. To store the model in a data set and use synchronization strategies, the Apache supplier is utilized. FREE Iris CASIA-V1 is utilized for recognition. The set of data comprises fifty individuals and five samples are taken in two sessions by each participant. For each module, we use four samples and a reference sample. Per sample is processed in a 320*280 JPG file. Table 1 describes the data collection and the system specification.

Table 1.3: Specification of data and machine

Microprocessor	Intel core-i7
Dataset	CASIA-V1 for IRIS
File format	Image JPG
Platform	Windows 10
Main Memory	8GB
Dimensions	320*280
Data size	5 images for each person We have 50 Persons

5.2 SAMPLE APPLICATION CODES

```
function [gradient, or] = canny(im, sigma, scaling, vert, horz)

xscaling = vert;
yscaling = horz;

hsize = [6*sigma+1, 6*sigma+1];   % The filter size.

gaussian = fspecial('gaussian',hsize,sigma);
im = filter2(gaussian,im);        % Smoothed image.

im = imresize(im, scaling);

[rows, cols] = size(im);

h =  [  im(:,2:cols)  zeros(rows,1) ] - [  zeros(rows,1)  im(:,1:cols-1)  ];
v =  [  im(2:rows,:); zeros(1,cols) ] - [  zeros(1,cols); im(1:rows-1,:)  ];
d1 = [  im(2:rows,2:cols) zeros(rows-1,1); zeros(1,cols) ] - ...
                               [ zeros(1,cols); zeros(rows-1,1) im(1:rows-1,1:cols-1)  ];
d2 = [  zeros(1,cols); im(1:rows-1,2:cols) zeros(rows-1,1);  ] - ...
                               [ zeros(rows-1,1) im(2:rows,1:cols-1); zeros(1,cols)   ];

X = ( h + (d1 + d2)/2.0 ) * xscaling;
Y = ( v + (d1 - d2)/2.0 ) * yscaling;

gradient = sqrt(X.*X + Y.*Y);
```

```
function [circleiris, circlepupil, imagewithnoise] = segmentiris(eyeimage)


%CASIA
lpupilradius = 28;
upupilradius = 75;
lirisradius = 80;
uirisradius = 150;

%    %LIONS
%    lpupilradius = 32;
%    upupilradius = 85;
%    lirisradius = 145;
%    uirisradius = 169;


% define scaling factor to speed up Hough transform
scaling = 0.4;

reflecthres = 240;

% find the iris boundary
[row, col, r] = findcircle(eyeimage, lirisradius, uirisradius, scaling, 2, 0.
```

```
function hd = gethammingdistance(temp1, mk1, temp2, mk2, scales)
template1 = importdata(fullfile(temp1));
mask1 = importdata(fullfile(mk1));
template2 = importdata(fullfile(temp2));
mask2 = importdata(fullfile(mk2));

template1 = logical(template1);
mask1 = logical(mask1);

template2 = logical(template2);
mask2 = logical(mask2);

hd = NaN;

% shift template left and right, use the lowest Hamming distance
for shifts=-8:8

    template1s = shiftbits(template1, shifts,scales);
    mask1s = shiftbits(mask1, shifts,scales);


    mask = mask1s | mask2;

    nummaskbits = sum(sum(mask == 1));

    totalbits = (size(template1s,1)*size(template1s,2)) - nummaskbit:
```

```
function im = nonmaxsup(inimage, orient, radius)

if size(inimage) ~= size(orient)
  error('image and orientation image are of different sizes');
end

if radius < 1
  error('radius must be >= 1');
end

[rows,cols] = size(inimage);
im = zeros(rows,cols);          % Preallocate memory for output image for speed
iradius = ceil(radius);

% Precalculate x and y offsets relative to centre pixel for each orientation angle

angle = [0:180].*pi/180;    % Array of angles in 1 degree increments (but in radians)
xoff = radius*cos(angle);   % x and y offset of points at specified radius and angle
yoff = radius*sin(angle);   % from each reference position.

hfrac = xoff - floor(xoff); % Fractional offset of xoff relative to integer location
vfrac = yoff - floor(yoff); % Fractional offset of yoff relative to integer location

orient = fix(orient)+1;     % Orientations start at 0 degrees but arrays start
                            % with index 1.

% Now run through the image interpolating grey values on each side
```

5.3 SYSTEM TESTING

- FAR: The chance to perceive a phony enrollment as a substantial enlistment.

$$FAR = \frac{\text{Number of Falsely accepted images}}{\text{Total number of imposter}} * 100\% \qquad (1)$$

- FRR: A chance to get to know a certified recorder as another option.

$$FRR = \frac{\text{Number of Falsely reject images}}{\text{Total number of genuine}} * 100\% \qquad (2)$$

- EER: Enter the sign when the FAR line meets the FRR line.

5.4 RESULTS

Subjection research is directed utilizing various deduction procedures, including straightforward mark discovering, PCA, SURF, SIFT, FSIFT. We used separate algorithms for each experiment. The measurement findings are presented in Table 5 for each trial. The FAR and FRR charts are presented in Figures 1,2 and 3 for each distance match algorithm. For each experiment, the time consuming map as shown in Figure 4.

Table 1.4: Precision and protection effects as various role extraction techniques are implemented using different algorithms.

Methods	Distance Measure	FRR %	FAR %	Required Time (sec)	Accuracy %
Canny Edge detection	Euclidean	0.0813	0.069	180	91
	Cosine	0.533	0.339	192	89
	Hamming	0.132	0.039	176	92
SIFT	Euclidean	0.036	0.0039	228	96
	Cosine	0.434	0.0244	280	94
	Hamming	0.031	0.0019	216	97
SURF	Euclidean	0.093	0.0052	178	95
	Cosine	0.152	0.0113	202	93
	Hamming	0.044	0.0022	158	96
PCA	Euclidean	0.081	0.0071	188	94
	Cosine	0.362	0.0250	212	90
	Hamming	0.088	0.0058	195	92
Fast SIFT	Euclidean	0.032	0.0042	118	97
	Cosine	0.073	0.0093	130	95
	Hamming	0.025	0.0015	103	98

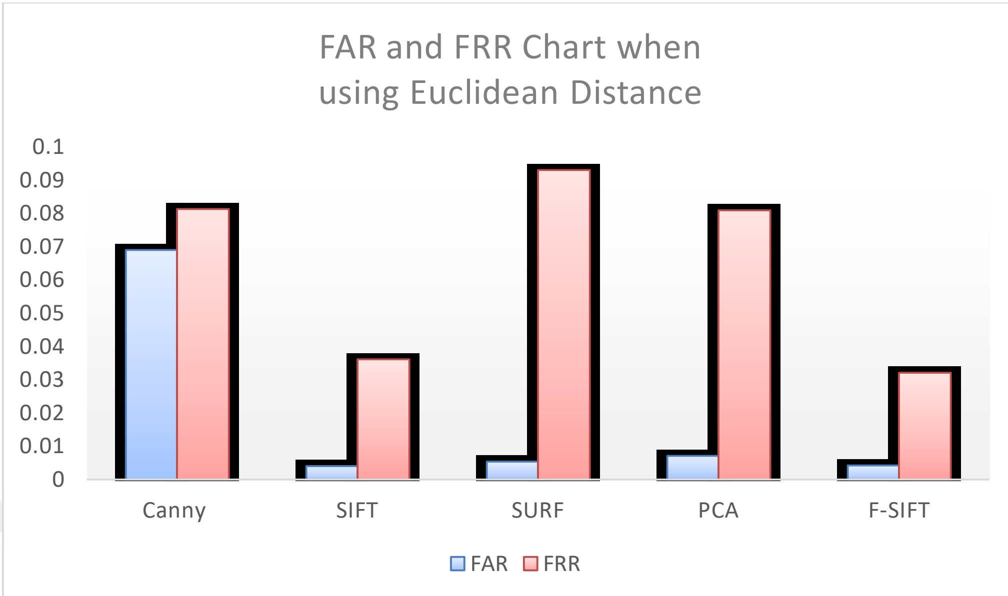

Figure 5.1: FAR and FRR assessment results dependent on Euclidean algorithm for each extraction function.

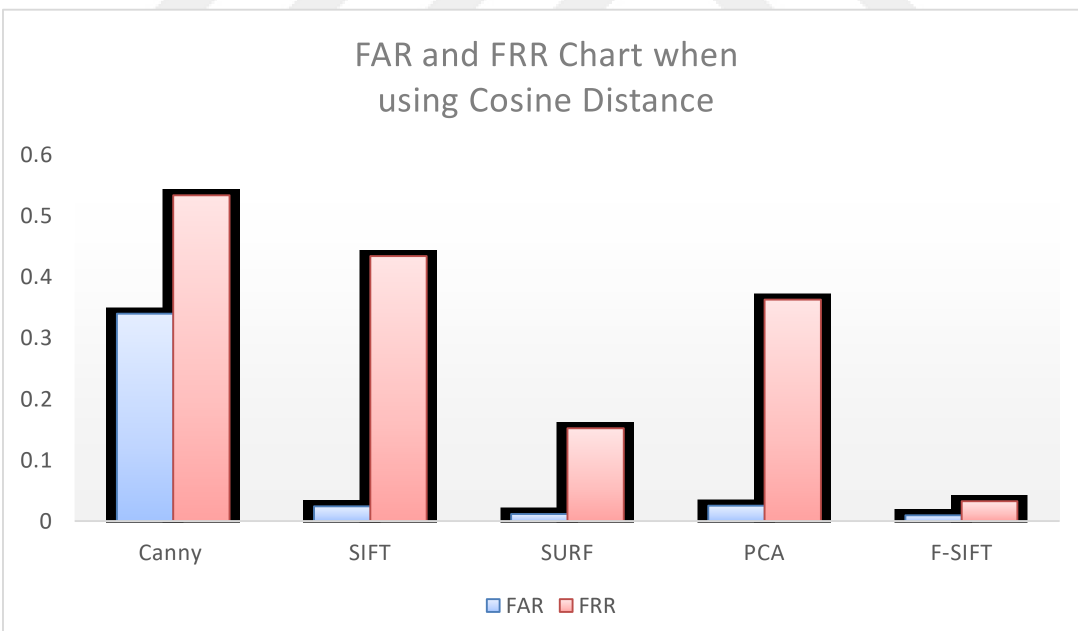

Figure 5.2: FAR and FRR evaluation outcomes dependent on a Cosine algorithm for each function extraction algorithm

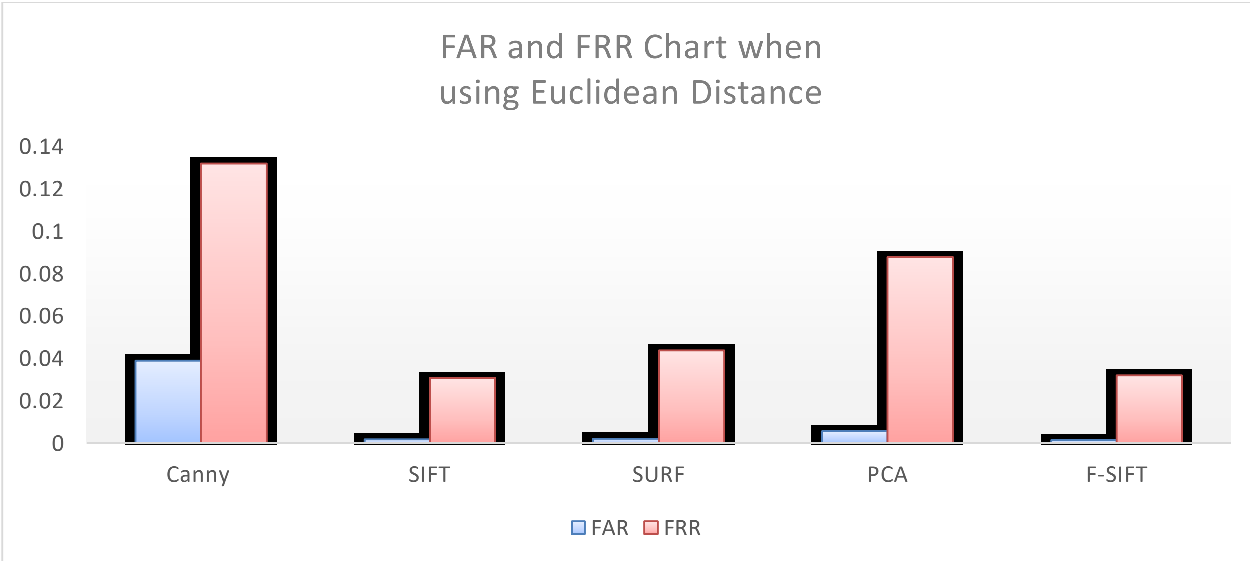

Figure 5.3: Evaluation FAR and FRR outcomes dependent on the Hamming algorithm for each extraction function

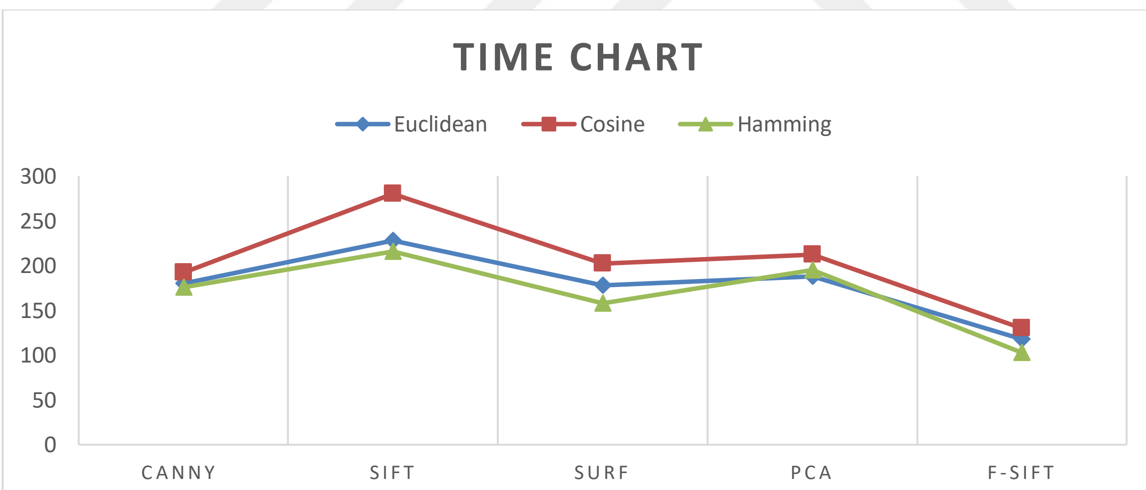

Figure 5.4: Results of time consumption for each extraction algorithm

6. CONCLUSIONS AND FUTURE WORK

6.1 CONCLUSIONS

A clever, single mode pattern recognition framework is proposed with different characteristic extraction and distance match algorithms to classify a person's identities. In this project. This innovation learns the exceptional iris examples and attributes of every person to manage an assortment of deterrents, like false ID, helpless picture quality, clamor, and climate stuns. Various expertise was conducted using the Hamming distance algorithm to evaluate the comparison of the individual to the previously entered data in a data collection comprising 50 individuals. With a false acceptability and false rejection rate of 0.0015% and 0.025%, the findings of the suggested method were 98% more accurate.

6.2 FUTURE WORK

This should encompass two fields: firstly, emerging research and development areas guided by the initiative and secondly, works that have not been finished owing to time limits and/or difficulties.

REFERENCES

[1] S.J. Savory, “Digital optical coherent receivers: algorithms and subsystems,” *IEEE J. Sel. Topics Quantum Electron.*, vol. 16, no. 5, pp. 1164- 1179, Sept./Oct. 2010.

[2] R.-J. Essiambre, G. Kramer, P.J. Winzer, G.J. Foschini and B. Goebel, “Capacity limits of optical fiber networks,” *IEEE/OSA J. Lightw. Technol.*, vol. 28, no. 4, pp. 662-701, Feb. 2010.

[3] L. Liu, L. Li, Y. Huang, K. Cui, Q. Xiong, F.N. Hauske, C. Xie and Y. Cai, “Interchannel nonlinearity compensation by inverse Volterra series transfer function,” *IEEE/OSA J. Lightw. Technol.*, vol. 30, no. 3, pp. 310-316, Feb. 2012.

[4] E. Ip, “Nonlinear compensation using backpropagation for polarizationmultiplexed transmission,” *IEEE/OSA J. Lightw. Technol.*, vol. 28, no. 6, pp. 939-951, Mar. 2010.

[5] W. Yan, Z. Tao, L. Dou, L. Li, S. Oda, T. Tanimura, T. Hoshida and J.C. Rasmussen, “Low complexity digital perturbation back-propagation,” *Proc. Opt. Fiber Commun. Conf (OFC)*, pp. Tu.3.A.2, Los Angeles, CA, USA, Mar. 2011.

[6] I. Fernandez de Jauregui Ruiz, A. Ghazisaeidi, G. Charlet, “Optimization rules and performance analysis of filtered digital backpropagation,” *Proc. Eur. Conf. Opt. Commun. (ECOC)*, pp. We.4.6.3, Valencia, Spain, Sept.- Oct. 2015.

[7] T. Tanimura, T. Hoshida, T. Tanaka, L. Li, S. Oda, H. Nakashima, Z. Tao, and J.C. Rasmussen, “Semi-blind nonlinear equalization in coherent multi-span transmission system with inhomogeneous span parameters,” *in Proc. Opt. Fiber Conf. (OFC)*, pp. OMR6, San Diego, CA, USA, Mar. 2010.

[8] A.J. Lowery, L.B. Du, and J. Armstrong, “Performance of optical OFDM in ultralong-haul WDM lightwave systems,” *IEEE/OSA J. Lightw. Technol.*, pp. 131-138, vol. 25, no. 1, Jan. 2007.

[9] A. Leven and L. Schmalen, “Status and recent advances on forward error correction technologies for lightwave systems,” *IEEE/OSA J. Lightw. Technol.*, pp. 2735-2750, vol. 32, no. 16, Aug. 2014.

[10] X. Li, A. Chindapol and J.A. Ritcey, “Bit-interleaved coded modulation with iterative decoding and 8-PSK signaling,” *IEEE Trans. Commun.*, pp. 1250-1257, vol. 50, no. 8, Aug. 2002.

[11] L. Kocarev, F. Lehmann, G.M. Maggio, B. Scanavino, Z. Tasev and A. Vardy, “Nonlinear dynamics of iterative decoding systems: analysis and applications,” *IEEE Trans. Inform. Theory*, vol.52, no. 4, pp. 1366-1384, Apr. 2006.

[12] R. Schmogrow, B. Nebendahl, M. Winter, A. Josten, D. Hillerkuss, S. Koenig, J. Meyer, M. Dreschmann, M. Huebner, C. Koos, J. Becker, W. Freude and J. Leuthold, “Error vector magnitude as a performance measure for advanced modulation formats,” *IEEE Photonics Technol. Lett.*, vol. 24, no. 1, pp. 61-63, Jan. 2012.

[13] P. P. Mitra and J. B. Stark, “Nonlinear limits to the information capacity of optical fibre communications,” *Nature*, vol. 411, pp. 1027–1030, 2001.

[14] D. Rafique, J. Zhao, and A. D. Ellis, “Digital back-propagation for spectrally efficient WDM 112 Gbit/s PM m-ary QAM transmission,” *Opt. Express*, vol. 19, pp. 5219–5224, 2011.

[15] G. Goldfarb, M. G. Taylor, and G. Li, “Experimental demonstration of fiber impairment compensation using the split-step finite-impulse-response filtering method,” *IEEE Photon. Technol. Lett.*, vol. 20, pp. 1887–1889, 2008.

[16] E. Ip and J. M. Kahn, “Compensation of dispersion and nonlinear impairments using digital backpropagation,” *J. Lightwave Technol.*, vol. 26, pp. 3416–3425, 2008.

[17] W. Shieh, H. Bao, and Y. Tang, “Coherent optical OFDM: Theory and design,” *Opt.Express*, vol. 16, pp. 841–859, 2008.

[18] L. B. Du and A. J. Lowery, “Improved single channel backpropagation for intrachannel fiber nonlinearity compensation in long-haul optical communication systems,” *Opt. Express*, vol. 18, pp. 17075–17088, 2010.

[19] B. Inan, S. Randel, S. L. Jansen, A. Lobato, S. Adhikari, and N. Hanik, “Pilottone-based nonlinearity compensation for optical OFDM systems,” in *Proc. European Conf. Optical Communication*, Torino, Italy, 2010, p. Tu.4.A.6.

[20] L. B. Du and A. J. Lowery, "Pilot-based cross-phase modulation compensation for coherent optical orthogonal frequency division multiplexing long-haul optical communications systems," *Opt. Lett*., vol. 36, pp. 1647–1649, 2011.

[21] K. Roberts, M. O'Sullivan, K.-T. Wu, H. Sun, A. Awadalla, D. J. Krause, and C. Laperle, "Performance of dual-polarization QPSK for optical transport systems," *J. Lightwave Technol*., vol. 27, pp. 3546–3559, 2009.

[22] M. Nazarathy, J. Khurgin, R. Weidenfeld, Y. Meiman, P. Cho, R. Noe, I. Shpantzer, and V. Karagodsky, "Phased-array cancellation of nonlinear FWM in coherent OFDM dispersive multi-span links," *Opt. Express*, vol. 16, pp. 15777–15810, 2008.

[23] E. Ip, "Nonlinear compensation using backpropagation for polarizationmultiplexed transmission," *J. Lightwave Technol*., vol. 28, pp. 939–951, 2010.

[24] D. Rafique and A. D. Ellis, "Various nonlinearity mitigation techniques employing optical and electronic approaches," *IEEE Photon. Technol. Lett.,* vol. 23, pp. 1838–1840, 2011.

[25] X. Chen and W. Shieh, "Closed-form expressions for nonlinear transmission performance of densely spaced coherent optical OFDM systems," *Opt. Express,* vol. 18, pp. 19039–19054, 2010.

[26] C. Paré, A. Villeneuve, P. A. Bélanger, and N. J. Doran, "Compensating for dispersion and the nonlinear Kerr effect without phase conjugation," *Opt. Lett.,* vol. 21, pp. 459–461, 1996.

[27] R. Killey, "Dispersion and nonlinearity compensation using electronic predistortion techniques," in *The IEE Seminar on Optical Fibre Communications and Electronic Signal Processing*. London, U.K.: IEE, 2005, pp. 0_14–2/6.

[28] R. Danish and D. E. Andrew, "The impact of signal-ASE four-wave mixing in coherent transmission systems," in *Proc. Optical Fiber Communication Conf.*, Los Angeles, California, 2011, p. OThO2.

[29] C. Xu and X. Liu, "Postnonlinearity compensation with data-driven phase modulators in phase-shift keying transmission," *Opt. Lett*., vol. 27, pp. 1619–1621, 2002.

[30] A. J. Lowery, “Fiber nonlinearity pre- and post-compensation for long-haul optical links using OFDM,” *Opt. Express*, vol. 15, pp. 12965–12970, 2007.

[31] L. B. Du and A. J. Lowery, “Improved nonlinearity precompensation for longhaul high-data-rate transmission using coherent optical OFDM,” *Opt. Express,* vol. 16, pp. 19920–19925, 2008.

[32] L. B. Du and A. J. Lowery, “Practical XPM compensation method for coherent optical OFDM systems,” *IEEE Photon. Technol. Lett*., vol. 22, pp. 320–322, 2010.

[33] L. Zhu and G. Li, “Folded digital backward propagation for dispersion-managed fiber-optic transmission,” *Opt. Express*, vol. 19, pp. 5953–5959, 2011.

[34] Z. Maalej, A. Napoli, V. Sleiffer, M. Kuschnerov, B. Spinnler, and N. Hanik, “Reduced complexity back-propagation for optical communication systems,” in *Proc. Optical Fiber Communication Conf. Expo./Nat. Fiber Optic Engineers Conf. (OFC/NFOEC)*, 2012, pp. 1–3.

[35] D. S. Millar, S. Makovejs, C. Behrens, S. Hellerbrand, R. I. Killey, P. Bayvel, and S. J. Savory, “Mitigation of fiber nonlinearity using a digital coherent receiver,” *IEEE Select. Topics Quantum Electron*., vol. 16, pp. 1217–1226, 2010.

[36] C. S. Fludger, T. Duthel, D. van den Borne, C. Schulien, E.-D. Schmidt, T. Wuth, J. Geyer, E. De Man, G.-D. Khoe, and H. de Waardt, “Coherent equalization and POLMUX-RZ-DQPSK for robust 100-GE transmission,” *J. Lightwave Technol.,* vol. 26, pp. 64–72, 2008.

[37] D. Rafique, M. Mussolin, M. Forzati, J. Mårtensson, M. N. Chugtai, and A. D. Ellis, “Compensation of intra-channel nonlinear fibre impairments using simplified digital back-propagation algorithm,” *Opt. Express*, vol. 19, pp. 9453–9460, 2011.

[38] S. L. Jansen, I. Morita, T. C. W. Schenk, N. Takeda, and H. Tanaka, “Coherent optical 25.8-Gb/s OFDM transmission over 4160-km SSMF,” *J. Lightwave Technol*., vol. 26, pp. 6–15, 2008.

[39] A. Diaz, A. Napoli, S. Adhikari, Z. Maalej, A. P. Lobato Polo, M. Kuschnerov, and J. Prat, “Analysis of back-propagation and RF pilot-tone based nonlinearity compensation for a 9x224Gb/s POLMUX- 16QAM system,” in *Proc. Optical Fibre Communication Conf.*, Los Angeles, California, 2012, p. OTh3C.5.

[40] L. B. Du and A. J. Lowery, “Pilot-based XPM nonlinearity compensator for COOFDM systems,” *Opt. Express*, vol. 19, pp. B862–B867, 2017.

[41] B. Spinnler, “Equalizer design and complexity for digital coherent receivers,” *IEEE Select. Topics Quantum Electron.*, vol. 16, pp. 1180–1192, 2015.

[42] S. J. Savory, G. Gavioli, E. Torrengo, and P. Poggiolini, “Impact of interchannel nonlinearities on a split-step intrachannel nonlinear equalizer,” *IEEE Photon. Technol. Lett.*, vol. 22, pp. 673–675,2017.

[43] L. Schmalen, A. Alvarado, and R. Rios-Muller, “Predicting the per- ̈ formance of nonbinary forward error correction in optical transmission experiments,” in *Optical Fiber Communication Conference (OFC)*, 2016, p. M2A.2.

[44] S. Beppu, K. Kasai, M. Yoshida, and M. Nakazawa, “2048 QAM (66 Gbit/s) single-carrier coherent optical transmission over 150 km with a potential SE of 15.3 bit/s/Hz,” *Opt. Express*, vol. 23, no. 4, pp. 4960–4969, Feb. 2015.

[45] D. Qian, E. Ip, M.-F. Huang, M.-J. Li, and T. Wang, “698.5-Gb/s PDM-2048QAM transmission over 3km multicore fiber,” in *Proc. European Conference on Optical Communication (ECOC)*, London, UK, Sep. 2013, p. Th.1.C.5.

[46] A. Alvarado, E. Agrell, D. Lavery, R. Maher, and P. Bayvel, “Replacing the soft-decision FEC limit paradigm in the design of optical communication systems,” *J. Lightw. Technol.*, vol. 33, no. 20, pp. 4338–4352, Oct. 2015, (Invited Paper).

[47] A. Guillen i F ́ abregas, A. Martinez, and G. Caire, “Bit-interleaved ̀ coded modulation,” *Foundations and Trends in Communications and Information Theory*, vol. 5, no. 1–2, pp. 1–153, 2008.

[48] L. Szczecinski and A. Alvarado, *Bit-Interleaved Coded Modulation: Fundamentals, Analysis and Design*. Chichester, UK: John Wiley & Sons, 2015.

[49] H. Bulow, ¨ U. Abay, A. Schenk, and J. B. Huber, "Coded modulation ¨ of polarization- and space-multiplexed signals," in *Proc. Asia Communications and Photonics Conference and Exhibition (ACP)*, Shanghai, China, Nov. 2011.

[50] A. Alvarado and E. Agrell, "Four-dimensional coded modulation with bit-wise decoders for future optical communications," *J. Lightw. Technol.*, vol. 33, no. 10, pp. 1993–2003, May 2015.

[51] I. B. Djordjevic and B. Vasic, "Nonbinary LDPC codes for optical communication systems," *IEEE Photon. Technol. Lett.*, vol. 17, no. 10, pp. 2224–2226, 2005.

[52] L. Beygi, E. Agrell, J. M. Kahn, and M. Karlsson, "Coded modulation for fiber-optic networks: Toward better tradeoff between signal processing complexity and optical transparent reach," *IEEE Signal Process. Mag.*, vol. 31, no. 2, pp. 93–103, 2014

[53] U. Wachsmann, R. F. H. Fischer, and J. B. Huber, "Multilevel codes: theoretical concepts and practical design rules," *IEEE Trans. Inf. Theory*, vol. 45, no. 5, pp. 1361–1391, 1999.

[54] A. Bisplinghoff, N. Beck, M. Ene, M. Danninger, and T. Kupfer, "Phase slip tolerant, low power multi-level coding for 64QAM with 12.9 dB NCG," in *Optical Fiber Communication Conference*. Optical Society of America, 2016, p. M3A.2

[55] G. Montorsi, "Analog digital belief propagation," *IEEE Commun. Lett.*, vol. 16, no. 7, pp. 1106–1109, Jul. 2012.

[56] M. Awais, G. Masera, M. Martina, and G. Montorsi, "VLSI implementation of a non-binary decoder based on the analog digital belief propagation," *IEEE Trans. Signal Process.*, vol. 62, no. 15, pp. 3965– 3975, Aug. 2014.

[57] M. Beermann, E. Monzo, L. Schmalen, and P. Vary, "GPU accelerated ´ belief propagation decoding of non-binary LDPC codes with parallel and sequential scheduling," *Journal of Signal Processing Systems*, vol. 78, no. 1, pp. 21–34, 2015.

[58] A. Leven, F. Vacondio, L. Schmalen, S. ten Brink, and W. Idler, “Estimation of soft FEC performance in optical transmission experiments,” *IEEE Photon. Technol. Lett.*, vol. 20, no. 23, pp. 1547–1549, 2011.

[59] M. Yankov, D. Zibar, K. Larsen, L. Christensen, and S. Forchhammer, “Constellation shaping for fiber-optic channels with QAM and high spectral efficiency,” *IEEE Photon. Technol. Lett.*, vol. 26, no. 23, pp. 2407–2410, Dec. 2014.

[60] T. Fehenberger, A. Alvarado, P. Bayvel, and N. Hanik, “On achievable rates for long-haul fiber-optic communications,” *Optics Express*, vol. 23, no. 7, pp. 9183–9191, 2015.